2018

Three-dimensional printing antimicrobial and radiopaque constructs

Christen J. Boyer
Louisiana State University Health Sciences Center - Shreveport

David H. Ballard
Washington University School of Medicine in St. Louis

Jeffery A. Weisman
Washington University School of Medicine in St. Louis

Spencer Hurst
Louisiana State University Health Sciences Center - Shreveport

David J. McGee
Louisiana State University Health Sciences Center - Shreveport

See next page for additional authors

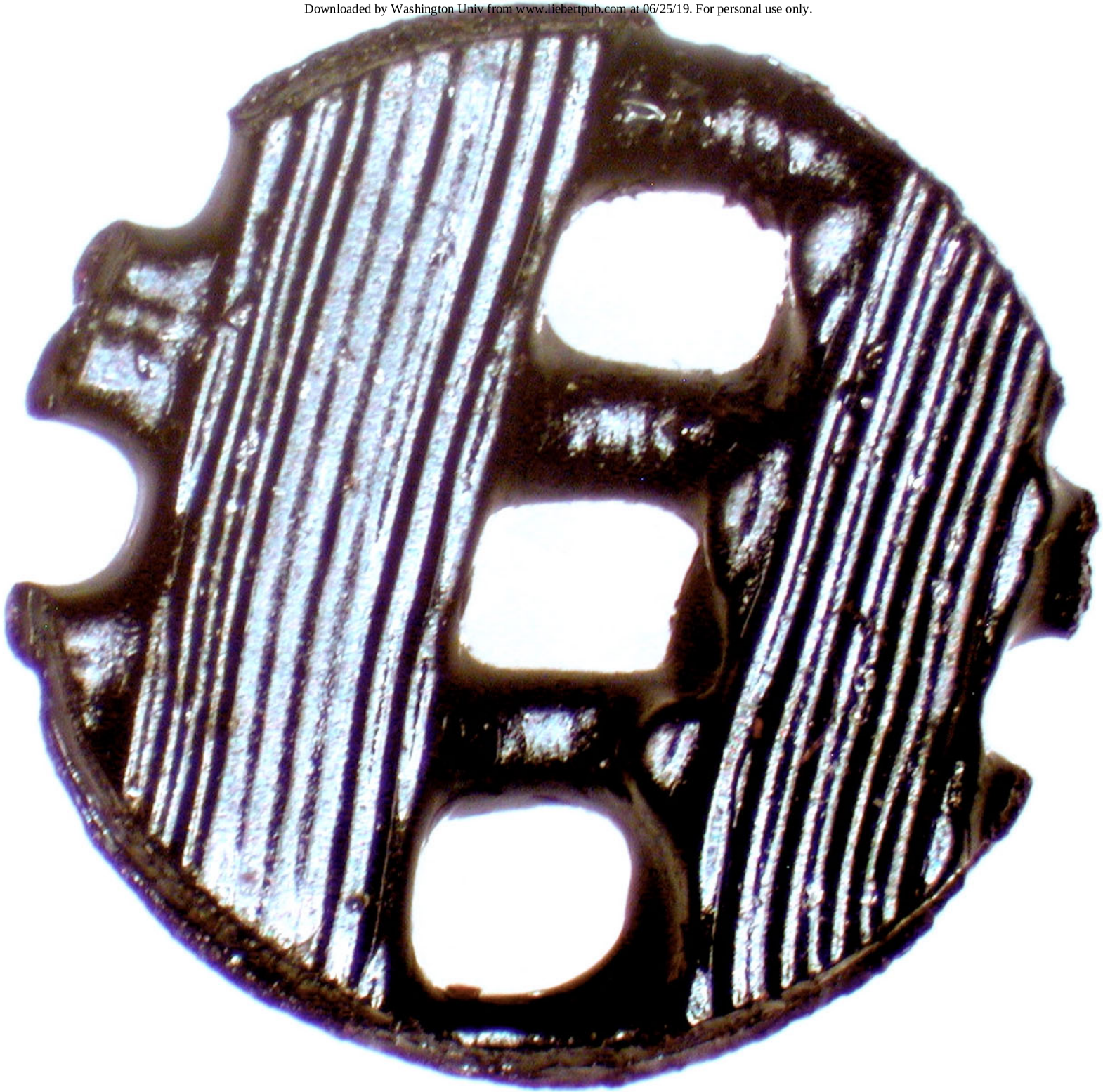

3D PRINTING AND ADDITIVE MANUFACTURING
Volume 5, Number 1, 2018

DOI: 10.1089/3dp.2017.0099

ORIGINAL ARTICLE

Three-Dimensional Printing Antimicrobial and Radiopaque Constructs

Christen J. Boyer,[1,2] David H. Ballard,[3] Jeffery A. Weisman,[4] Spencer Hurst,[1] David J. McGee,[5] David K. Mills,[6] Jennifer E. Woerner,[2] Uday Jammalamadaka,[3] Karthik Tappa,[3] and Jonathan Steven Alexander[1]

Abstract

Three-dimensional (3D) printing holds tremendous potential as a tool for patient-specific devices. This proof-of-concept study demonstrated the feasibility, antimicrobial properties, and computed tomography (CT) imaging characteristics of iodine/polyvinyl alcohol (PVA) 3D meshes and stents. Under scanning electron microscopy, cross-linked PVA displays smoother and more compacted filament arrangements. X-ray and transaxial CT images of iodized PVA vascular stents show excellent visibility and significantly higher Hounsfield units of radiopacity than control prints. Three-dimensional PVA prints stabilized by glutaraldehyde cross-linking and loaded with iodine through sublimation significantly suppressed *Escherichia coli* and *Staphylococcus aureus* growth in human blood agar disk diffusion assays. It is suggested that PVA 3D printing with iodine represents an important new synthetic platform for generating a wide variety of antimicrobial and high-visibility devices.

Keywords: three-dimensional printing, personalized medicine, antimicrobials, iodinated contrast, computed tomography

Introduction

Three-dimensional (3D) printing with antimicrobial properties is still in its infancy, with only a limited number studies published that demonstrate the potential of 3D-printed antimicrobial materials.[1–6] Many recent antibacterial 3D printing methods have focused on preprint loading methods, including surface coatings, preloaded filaments, and resins. By comparison, iodine has been used as an effective antimicrobial wound care agent for >180 years, and adaptation of new fabrication technologies that incorporate iodine may offer potent and novel anti-infective strategies.[7]

Polymer–iodine complexes, known as *iodophors*, are currently in use as antiseptics and in wound care dressings to prevent infection.[8–11] Povidone iodine (PVP-I) is one of the most widely used iodophors, and *in vitro* and *in vivo* studies have long demonstrated that PVP-I is highly effective against a broad spectrum of bacterial wound isolates and even antibiotic-resistant species.[12–16] PVP-I is available in many different formulations including solutions, creams, ointments, sprays, and wound dressings and there is evidence that PVP-I may even improve wound healing. In one human case study, PVP-I significantly increased the healing rate and reduced healing time in leg ulcers compared with other conventional antiseptics (silver sulfadiazine and chlorhexidine digluconate).[14]

This research explored a similar polymer, polyvinyl alcohol (PVA), as a custom 3D print platform for iodization. PVA is a multifunctional polymer, compatible with 3D printing techniques, such as fused deposition modeling. Importantly, PVA is a water soluble synthetic polymer, similar to PVP, which is capable of forming a molecular inclusion complex with iodine. PVA loaded with iodine (PVA-I) has already been used effectively in iodized foams in wound care management and has a unique color change property that allows for visual detection of iodine depletion.[17] Iodized

Departments of [1]Molecular and Cellular Physiology and [2]Oral and Maxillofacial Surgery, Louisiana State University Health Sciences Center, Shreveport, Louisiana.
[3]Mallinckrodt Institute of Radiology and [4]Department of Anesthesiology, Washington University School of Medicine, St. Louis, Missori.
[5]Department of Microbiology and Immunology, Louisiana State University Health Sciences Center, Shreveport, Louisiana.
[6]School of Biological Sciences, Louisiana Tech University, Ruston, Louisiana.

Opposite page: Crosslinked and iodized three-dimensionally printed polyvinyl alcohol. *Photo Credit:* Christen Boyer.

PVA materials are initially black/brown and as the iodine is depleted, the scaffold returns to its natural color, which ranges from clear to a cream yellow.

Iodine is also widely applied as an intravascular contrast agent used for computed tomography (CT), angiography, and fluoroscopy imaging due to its intrinsic ability to attenuate X-radiation.[18] Incorporation of iodine has been used in experimental settings for some time in construction of various polymers with the purpose of increasing or facilitating radiodensity.[19–21]

Reports show that constructed embolic materials (tested in sheep aortas) demonstrate excellent visibility.[19] A variety of different iodine containing polymers were tested within sheep aortas and their visibility was determined both by spectroscopy and by fluoroscopic observation.[19] They concluded that specific isomers of iodine (4-iodo- and 2,3,5-triiodobenzoyl) along with esters synthesized in cellulose achieved high iodine concentrations and radiopacity, whereas isomers and solvents that failed to sufficiently incorporate iodine did not achieve radiopacity.[19] Despite these findings, iodine-containing temporary or permanent medical implants are not yet extensively used in clinical practice, reflecting concerns about local and systemic toxicity as well as contrast-induced nephropathy.[22,23]

Although there is abundant evidence to support these types of iodophors as effective antimicrobial agents, some clinicians have expressed reluctance over iodine's cytotoxicity, which depends on iodophor concentration and the rate and mechanism of iodine release.[17] Advanced technologies, such as 3D printing, may overcome many of these issues through localizing iodine delivery, allowing for more customized wound care scaffolds to be fabricated to patient-specific anatomies, and adjusting iodine-dosing concentrations tailored to the nature of the wound, type, and size.

In this study, we successfully 3D-printed PVA devices, cross-linked the PVA, and then iodized the prints through gaseous sublimation. This approach provides a highly accessible, inexpensive, and ''tunable'' architecturally diverse synthetic platform for producing antimicrobial and radiopaque devices and meshes.

Materials and Methods

Synthesis of iodized PVA scaffolds

PVA filaments (AquaSolve™, Formfutura, Nijmegen, The Netherlands, 1.75 mm diameter) were 3D printed into mesh patterns at 201°C using a consumer grade MakerBot replicator desktop 3D printer (MakerBot Industries LLC, Brooklyn, NY). For control and experimental samples, circular disks (6.0 mm diameter and 0.8 mm thickness) were cut from the 3D-printed meshes using a sterile hole punch before iodine loading, electron microscopy, and agar disk diffusion antibacterial assays. Additional PVA samples were immersed in distilled water, dried at 25°C (1 h), and cross-linked by placing the PVA models in a gas vapor desiccator containing two separate 50 mL containers containing (1) 20 mL of 4% glutaraldehyde (GA) (EMD Millipore Corporation, Darmstadt, Germany) and (2) 10 mL of concentrated hydrochloric acid (Fisher Scientific, Hampton, NH) at 42°C for 24 h.

Cross-linked PVA scaffolds were then rinsed extensively in distilled water and air dried for 24 h. For iodine loading, PVA and cross-linked PVA (PVA-X) meshes were placed in a closed 20 mL volume glass chamber containing 110 mg of iodine crystals (Mallinckrodt Pharmaceuticals, St. Louis, MO). The samples were incubated at 42°C for 24 h to produce gaseous iodine through sublimation, which generated PVA-I and PVA-X loaded with iodine (PVA-X-I). Iodized samples were next removed from the chamber and air dried for 24 h. Vascular Y-stents were also printed with PVA and subjected to the same cross-linking and iodine-loading procedures for CT imaging.

Scanning electron microscopy and X-radiation imaging

Three-dimensional printed surface topographies were characterized with an S-4800 field-emission scanning electron microscope (SEM) (HITACHI, Tokyo, Japan). Samples were mounted on double-sided adhesive carbon tape and attached to the working stage. X-ray imaging was accomplished using an OEC 9900 Elite C-Arm System by General Electric (Fairfield, CT).

Image acquisition with CT

Transaxial CT images of the iodine-impregnated scaffolds of simulated Y-vascular stents were acquired using a Siemens Biograph PET/CT scanner (Siemens, Munich, Germany) with 120 kVp and slice thickness of 0.6 mm. Coronal and sagittal reconstructions were constructed at the image acquisition workstation. Images were analyzed using Osirx (Pixmeo SARL, Bernex, Switzerland) and Vitrea Enterprise Suite (Vital Images, Inc., Minnetonka, MN). Hounsfield units (HU) of each scaffold were measured using a small elliptical region of interest. Three HU were acquired for each of the four scaffolds. Mean HU for each scaffold were compared with one another using Student's *t*-test.

Evaluation of antimicrobial potential of iodized PVA scaffolds

Escherichia coli and *Staphylococcus aureus* were used to create 0.5 McFarland standard bacterial suspensions, and 50 μL of suspension was added to human blood agar plates for incubation with samples. Each series was tested in triplicate and incubated for 24 h at 37°C. Paper disks were loaded with 10 μL of Triadine PVP-I solution (Triad Group, Inc., Brookfield, WI) and also tested with 3D-printed samples. For all disk diffusion assays, the bacterial zones of inhibition (ZOI) were measured with a digital caliper. Mean ZOI for each sample type were compared with one another using Student's *t*-test for both *E. coli* and *S. aureus*.

Results

Cross-linking effect on 3D-printed PVA surfaces

The utility of iodine gas sublimation as a 3D-printed PVA surface modification with antibacterial properties was confirmed in a series of experiments designed to characterize its material properties, interface, and antibacterial inhibitory responses to Gram-negative and Gram-positive bacteria. SEM micrographs showed a smoother and more compact filament topography in cross-linked PVA polymer networks than in the noncross-linked PVA polymer networks (Fig. 1A–D). The iodized PVA prints were also shown to be radiopaque when viewed under X-ray imaging (Fig. 2A, B).

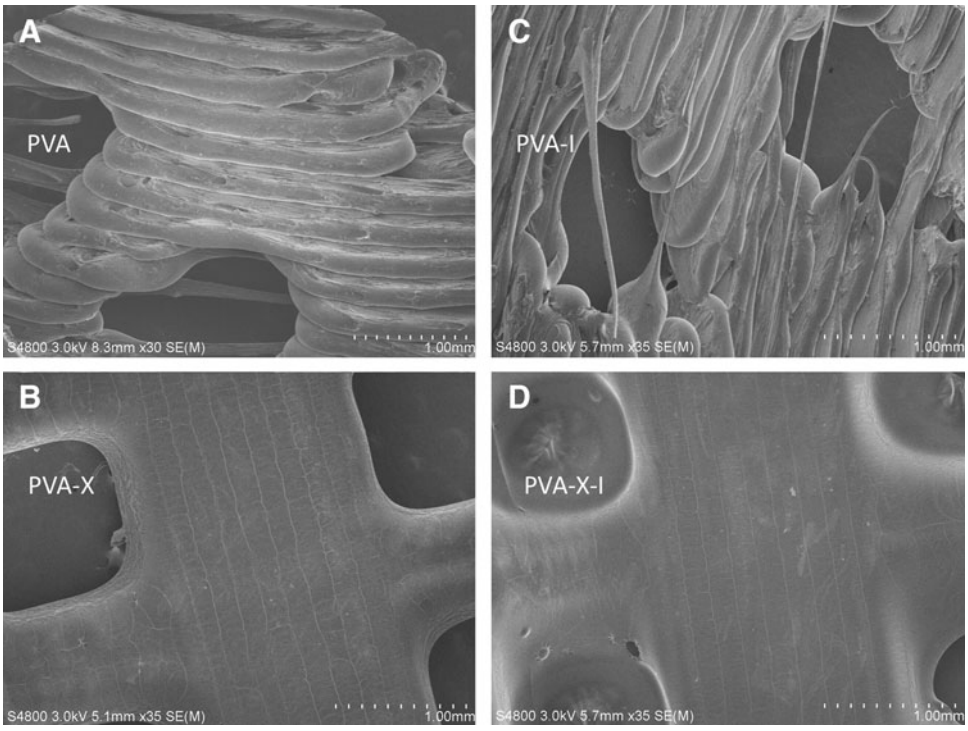

FIG. 1. Scanning electron microscopic images of **(A)** PVA, **(B)** PVA-X, **(C)** PVA-I, and **(D)** PVA-X-I. PVA, polyvinyl alcohol; PVA-X, cross-linked PVA; PVA-I, PVA loaded with iodine; PVA-X-I, PVA-X loaded with iodine.

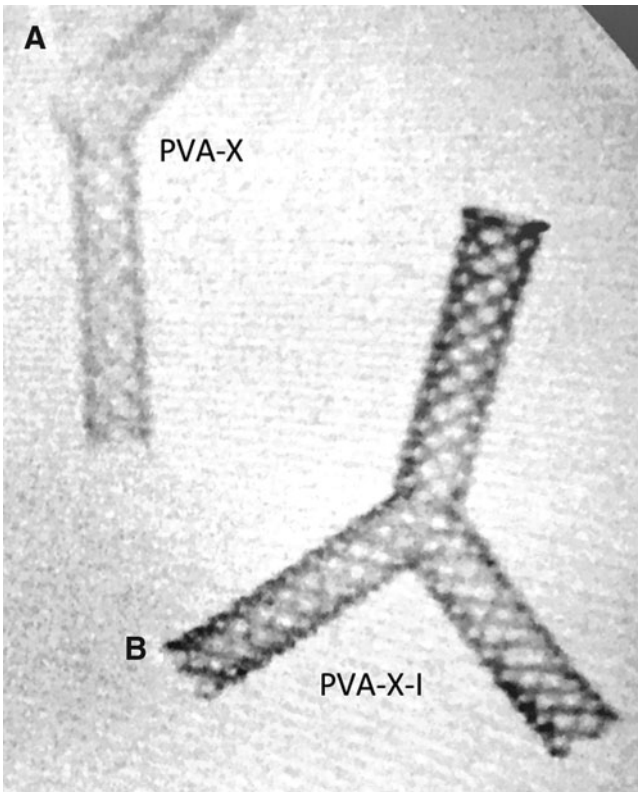

FIG. 2. X-ray images of **(A)** PVA-X and **(B)** PVA-X-I.

Imaging capability of 3D PVA stents

For imaging studies, vascular Y-stents made of PVA-I and PVA-X-I were evaluated and found to be dense and readily visible by CT. By comparison, PVA and PVA-X were significantly less dense and required windowing to achieve visibility on CT (Fig. 3). Quantitatively, PVA-I and PVA-X-I were found to have significantly higher HU than PVA and PVA-X (1666.3 and 1120.7 HU vs. 10.7 and 63.0 HU; $p < 0.0001$ in both comparisons). PVA-I mean HU of 1666.3 were significantly higher than PVA-X-I mean HU (mean HU 1120.7; $p < 0.0001$). There was no significant difference in HU with PVA compared with PVA-X ($p = 0.10$).

Effect of 3D PVA type on bacteria growth

For antibacterial testing, PVA-I and PVA-X-I were found to release sufficient iodine to inhibit both Gram-negative and Gram-positive bacterial growth during agar disk diffusion assays (Fig. 4). For all experiments, the PVA and PVA-I fully dissolved, whereas the PVA-X and PVA-X-I versions maintained hydrogel cross-linked formations. PVA-I meshes inhibited bacterial growths with a mean ± standard deviation ZOI of 11.70 ± 0.50 mm ($n = 3$) for *E. coli* and 13.63 ± 0.58 mm ($n = 3$) for *S. aureus*. PVA-X-I meshes inhibited bacterial growth with a mean ± standard deviation ZOI of 12.76 ± 1.06 mm ($n = 3$) for *E. coli* and 12.70 ± 0.60 mm ($n = 3$) for *S. aureus*. PVA and PVA-X displayed no ZOI. The PVP-I inhibited bacterial growth with a mean ± standard deviation ZOI of 8.20 ± 0.04 mm ($n = 6$) for *E. coli* and 8.88 ± 0.65 mm ($n = 6$) for *S. aureus*.

When compared with PVP-I filter paper disks, all samples (PVA, PVA-X, PVA-I, and PVA-X-I) were significantly

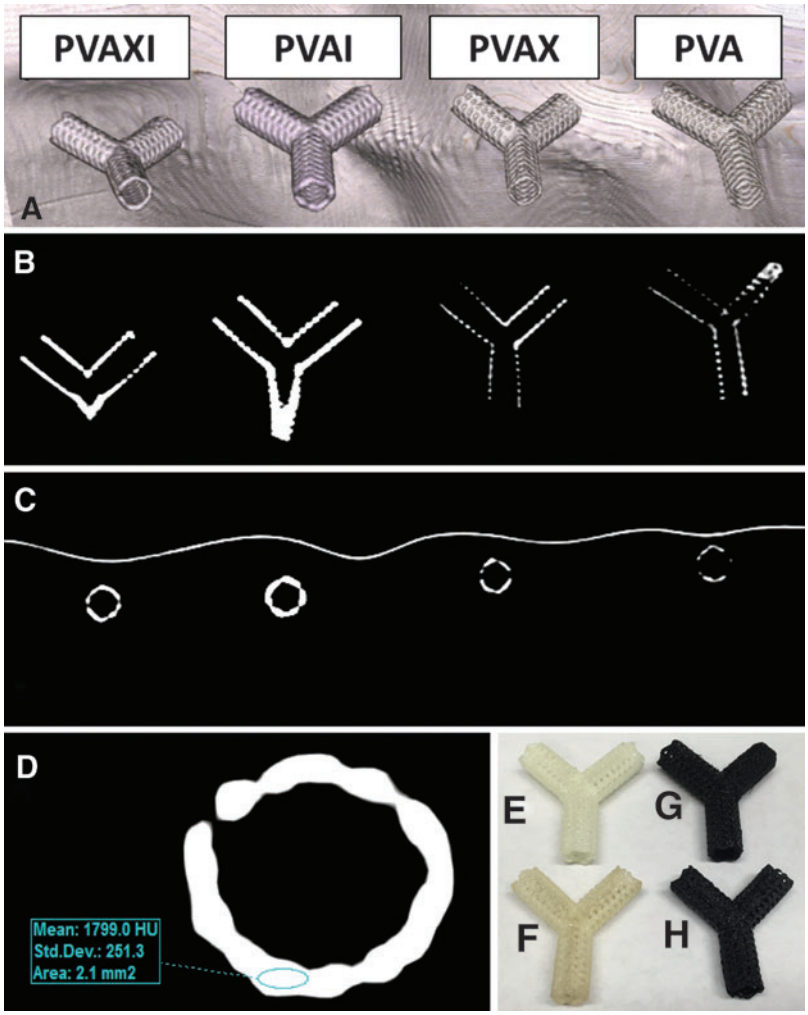

FIG. 3. CT image acquisition of iodine-impregnated and control 3D-printed vascular Y-stent substrates **(A–C)**. Transaxial **(A)** CT images of the 3D-printed substrate with coronal **(B)** and 3D coronal reconstructions. **(D)** Illustration of acquiring the Hounsfield units data using an elliptical region of interest on the PVA-I stent. Color image displaying **(E)** PVA, **(F)** PVA-X, **(G)** PVA-I, and **(H)** PVA-X-I stents. Color images available online at www.liebertpub.com/3dp

different ($p < 0.0001$). For PVA-I versus PVA-X-I, no significant differences were found for the ZOI (*E. coli* $p = 0.1923$, *S. aureus* $p = 0.1141$). For the PVA versus PVA-I ZOI, there were significant differences for both *E. coli* and *S. aureus* ($P < 0.0001$). For the PVA-X versus PVA-X-I, significant differences were also noted for both *E. coli* and *S. aureus* ($p < 0.0001$).

Discussion

Three-dimensional printing techniques have already enormous utility in many industrial applications and are viewed as important tools in future clinical technology development. Medical applications for 3D printing are rapidly expanding and soon may replace many conventional biomaterial manufacturing approaches, as customizable and on-demand wound care products with localized drug delivery have many diverse applications.[24] A wide range of materials are being explored for medical applications in 3D printing, which include plastics, metals, ceramics, and biological materials.[25] The current era of rapid prototyping and the rapidly expanding catalog of compatible materials are expanding the potential for new tissue and organ fabrication techniques in transplantation, as well as new pharmaceuticals and drug delivery systems.[26,27]

Iodine-containing 3D-printed scaffolds were found to have significantly higher HU and demonstrated superior visibility on CT. Although the iodine-containing scaffolds without cross-linking (PVA-I) had significantly higher HU (than the cross-linked iodine-containing scaffolds (PVA-X-I), this is not likely to be highly meaningful clinically as both were well visible (i.e., highly radiodense) on CT. In this study, we choose an atypical configuration of a vascular stent (Y-stent) as a proof on principle and to add dimensions/complexity to our 3D-printed constructs. In this format, the principle of iodine-containing customizable devices again demonstrates the value of iodination in custom-constructed 3D-printed implants.

Therefore, in addition to radiopacity, the iodination of implants (e.g., vascular stents) may create materials that have the ability to reduce or eliminate colonization with bacteria (i.e., ''nidus'' of infection) and to reduce the risk of localized infection associated with implantation of foreign materials.

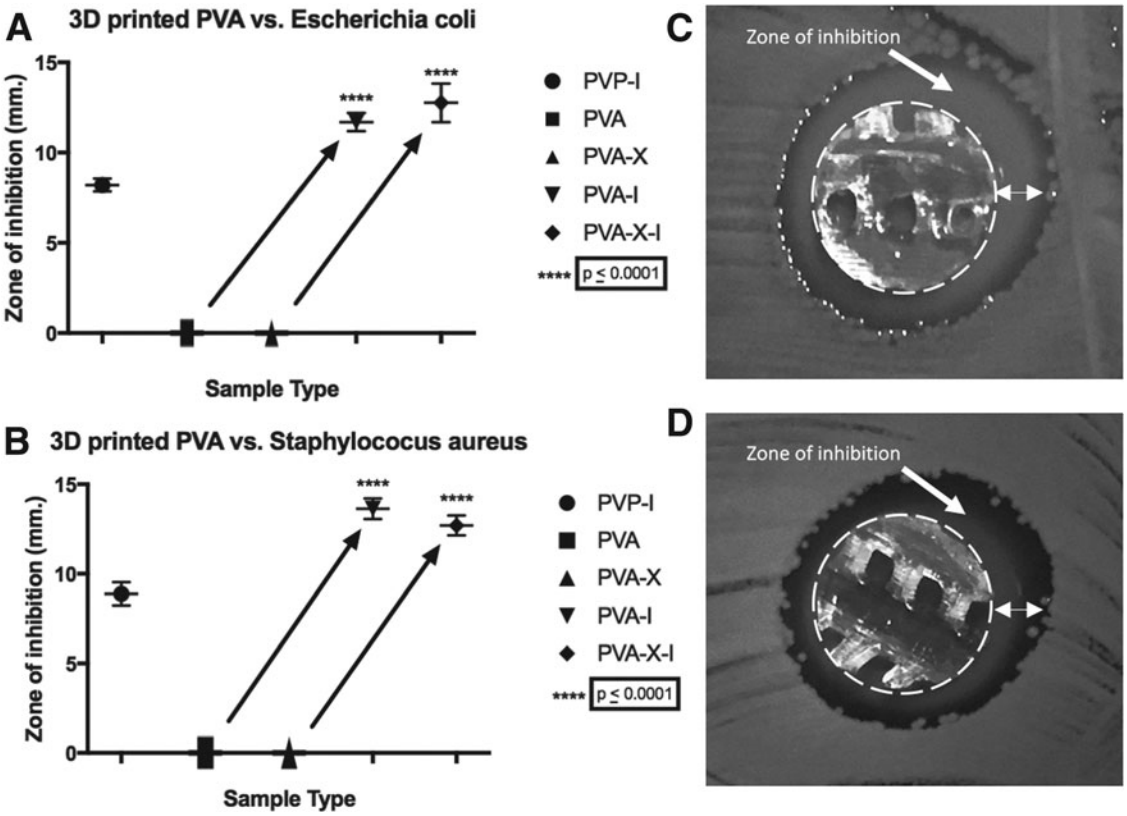

FIG. 4. Charts displaying the zones of inhibition for substrates against **(A)** *Escherichia coli* and **(B)** *Staphylococcus aureus* in blood agar disk diffusion assays. Images show 3D-printed PVA-X-I samples in blood agar disk diffusion assays against **(C)** *E. coli* and **(D)** *S. aureus*. The *dotted circle* in **(C)** and **(D)** represents the 3D print perimeter and the *double-headed arrow* represents the zone of inhibition.

Three-dimensional printing offers the ability to fabricate custom implants with tailored concentrations of iodinated material for imaging and antimicrobial applications.

The nature of additive manufacture is such that an iodine-containing layer can be created within the scaffold for extended release or long-term imaging. Through additional polymer coatings, which can be permanent or slow degrading, the iodine prints can be shielded from the outside (reducing toxicity). These additional layers and porous scaffolds can potentially provide more surface area to increase or customize the overall iodine content of a given construct. If a construct is impregnated with iodine for imaging purposes only, the deeper filaments can have higher concentrations of iodine, whereas the more superficial layers could be manufactured with lower concentrations or even completely free of iodine.

Alternatively, if elution of iodine is desired, iodine concentration can be maintained uniform throughout the construct. With bioabsorbable plastics, this would potentially unmask a ''new'' coating of iodine every time the most superficial layer dissolves.[6,28] In addition, the use of iodine sublimation with printed PVA matrixes allows derivatization in solid phase and avoids the need for aqueous I_2/KI mixtures that might dissolve or warp these matrices. Although iodine complexed with PVA in this manner may have antimicrobial and visibility properties, testing of this material is needed to determine any limitations to its practical applications for routine clinical use.

Although nephrotoxicity associated with iodinated intravascular contrast media is well described, recent data suggest its warnings may have somewhat overestimated risk compared with prior estimates.[22,23] Imaging of iodine diffusion into adjacent tissues might be used to measure iodine abundance, also may be advantageous in nonvascular antimicrobial applications (e.g., iodine-impregnated devices in a nonvascular postoperative cavity).

The refinements of 3D-printed implant approaches will allow their introduction into clinical practice; however, they are not yet well defined, especially with bioactive printing (i.e., impregnating drugs or compounds into an implant or instrument's structure). The United States Food and Drug Administration has published its own perspectives on this topic, addressing known and unknown issues regarding regulation of 3D-printed materials within medical use.[29] Although 3D-printed models and some implants have demonstrated value by reducing operating room time,[30,31] more research is needed to validate this, especially when considering bioactive 3D printing, which has not been extensively evaluated in humans at the time of writing.[28]

In this study, we did not study the effect of sterilization techniques and their potential effect on the composition of the iodine-containing substrates. Options for printing sterile implants in 3D printing include printing all material in a sterile environment or chemical sterilization, with compounds such as GA.[28,32] Another limitation to applying the present data and

concepts in animals or humans is that it is unknown whether the visibility in the constructs will be maintained over time, after implantation. Future study designs in animals or humans should obtain initial imaging and compare the visibility or HU with imaging taken over several days to weeks. In addition, *in vivo* implantation may have an immediate effect on X-ray attenuation compared with the *in vitro* data obtained in this study.

Commercial iodine wound dressing materials have been previously studied with various microorganisms.[33] The mean ZOI reported for iodine dressings against *S. aureus* was 14 mm, which suggests that 3D-printed PVA-I and PVA-X-I are comparable with commercial grade wound dressings and hold tremendous potential in antimicrobial applications.[33]

Conclusions

To our knowledge, this is the first report showing that post-3D-printed materials can be loaded with iodine through sublimation to exhibit microbiostatic and radiopaque properties. The sublimation process produced molecular iodine gas, which reacted with the PVA hydroxyl groups to form PVA iodine complexes. It is apparent that GA cross-linking appears to reduce at least some of potential binding sites where iodine interacts with PVA; however, cross-linking generates a PVA hydrogel scaffold with much greater hydrophilic lifetime, enabling extended release. Using this method, we anticipate that a large variety of wound care products may be fabricated that can be modified for localized delivery of different rates of iodine release with different intensities of antimicrobial activity.

The realization of scalable and cost-effective antimicrobial biomaterial fabrication techniques may provide clinicians with a new and powerful arsenal of antimicrobial materials. These methods may also be potentially used with larger custom sublimation chambers to synthesize iodized 3D-printed PVA objects at an industrial-scale amount or produce relatively smaller in-house productions at healthcare facilities. Overall, the iodized 3D print created through sublimation provides a foundation for future researchers to explore and has potential uses as medical devices, wound dressings, and antimicrobial surfaces.

Acknowledgments

The authors would like to thank Louisiana State University Health Sciences Center Shreveport for supporting this research and Washington University School of Medicine for CT usage.

Author Disclosure Statement

The authors have no conflicts of interest to disclose.

References

1. Weisman JA, Nicholson JC, Tappa K, Jammalamandaka U, *et al.* Antibiotic and chemotherapeutic enhanced three-dimensional printer filaments and constructs for biomedical applications. Int J Nanomed 2015;10:357–370.
2. Yue J, Zhao P, Gerasimov J, *et al.* 3D-printable antimicrobial composite resins. Adv Funct Mater 2015;25:6756–6767.
3. Sandler N, Salmela I, Fallarero A, *et al.* Towards fabrication of 3D printed medical devices to prevent biofilm formation. Int J Pharm 2014;459:62–64.
4. Wu CS. Modulation, functionality, and cytocompatibility of three-dimensional printing materials made from chitosan-based polysaccharide composites. Mater Sci Eng C 2016;1: 27–36.
5. Yang Y, Yang S, Wang Y, *et al.* Anti-infective efficacy, cytocompatibility and biocompatibility of a 3D-printed osteoconductive composite scaffold functionalized with quaternized chitosan. Acta Biomater 2016; 46:112–128.
6. Ballard DH, Weisman JA, Jammalamandaka U, *et al.* Three-dimensional printing of bioactive hernia meshes: In vitro proof of principle. Surgery 2017;161:1479–1481.
7. Hugo WB. A brief history of heat and chemical preservation and disinfection. J Appl Bacteriol 1991;71;9–18.
8. Zhou LH, Nahm WK, Badiavas E, *et al.* Slow release iodine preparation and wound healing: In vitro effects consistent with lack of in vivo toxicity in human chronic wounds. Br J Dermatol 2002;146:365–374.
9. Lamme EN, Gustafsson TO, Middelkoop E. Cadexomer iodine shows stimulation of epidermal regeneration in experimental full thickness wounds. Arch Dermatol Res 1998;290:18–24.
10. Mertz PM, Oliveira-Gandia MF, Davis SC. The evaluation of a cadexomer iodine wound dressing on methicillin resistant Staphylococcus aureus (MRSA) in acute wounds. Dermatol Surg 1999;25:89–93.
11. Leaper DJ. Leading article. Surgical site infection. Br J Surg 2010;97:1601–1602.
12. Lawrence J. A povidone iodine medicated dressing. J Wound Care 1998;7:332–336.
13. Schreier H, Erdos G, Reimer K, *et al.* Molecular effects of povidone-iodine on relevant micro-organisms: An electron-microscopic and biochemical study. Dermatology 1997;195: 111–116.
14. Fumal I, Braham C, Paquet P, *et al.* The beneficial toxicity paradox of antimicrobials in leg ulcer healing impaired by a polymicrobial flora: A proof-of-concept study. Dermatology 2002;204:70–74.
15. Giacometti A, Cirioni O, Greganti G, *et al.* Antiseptic compounds still active against bacterial strains isolated from surgical wound infections despite increasing antibiotic resistance. Eur J Clin Microbiol Infect Dis 2002; 21:553–556.
16. McLure AR, Gordon J. In vitro evaluation of povidone-iodine and chlorhexidine against methicillin-resistant *Staphylococcus aureus*. J Hosp Infect 1992;21:291–299.
17. Drosou A, Falabella A, Kirsner RS. Antiseptics on wounds: An area of controversy. Wounds 2003;15:149–166.
18. Lee N, Choi SH, Hyeon T. Nano-sized CT contrast agents. Adv Mater 2013;25:2641–2660.
19. Mottu F, Rüfenacht DA, Laurent A, *et al.* Iodine-containing cellulose mixed esters as radiopaque polymers for direct embolization of cerebral aneurysms and arteriovenous malformations. Biomaterials 2002;23:121–131.
20. Aviv H, Bartling S, Kieslling F, *et al.* Radiopaque iodinated copolymeric nanoparticles for X-ray imaging applications. Biomaterials 2009;30:5610–5616.
21. Samuel R, Girard E, Chagnon G, *et al.* Radiopaque poly (ε-caprolactone) as additive for X-ray imaging of temporary implantable medical devices. R Soc Chem Adv 2015;5: 84125–84133.

22. McDonald RJ, McDonald JS, Bida JP, *et al.* Intravenous contrast material-induced nephropathy: Causal or coincident phenomenon? Radiology 2013;267:106–118.
23. McDonald JS, McDonald RJ, Comin J, *et al.* Frequency of acute kidney injury following intravenous contrast medium administration: A systematic review and meta-analysis. Radiology 2013;267:119–128.
24. Mamidwar S, Hodge S, Deshmukh V, *et al.* Hot-melt extrusion. Int J Pharm Sci Rev Res 2012;15:105–112.
25. Gross BC, Erkal JL, Lockwood SY, *et al.* Evaluation of 3D printing and its potential impact on biotechnology and chemical sciences. Anal Chem 2014;86:3240–3253.
26. Marro A, Bandukwala T, Mak W. Three-dimensional printing and medical imaging: A review of the methods and applications. Curr Probl Diagn Radiol 2016;45:2–9.
27. Teo EY, Ong SY, Chong MS, *et al.* Polycaprolactone-based fused deposition modeled mesh for delivery of antibacterial agents to infected wounds. Biomaterials 2011;32:279–287.
28. Ballard DH, Trace AP, Ali S, *et al.* Clinical applications of 3D printing: Primer for radiologists. Acad Radiol 2018;25:52–65.
29. Di PM, Coburn J, Hwang D, *et al.* Additively manufactured medical products–the FDA perspective. 3D Printing Med 2015;2:1.
30. Tack P, Victor J, Gemmel P, *et al.* 3D-printing techniques in a medical setting: A systematic literature review. Biomed Eng Online 2016;15:115.
31. Martelli N, Serrano C, Van Den Brink H, *et al.* Advantages and disadvantages of 3-dimensional printing in surgery: A systematic review. Surgery 2016;159:1485–1500.
32. Rankin TM, Giovinco NA, Cucher DJ, *et al.* Three- dimensional printing surgical instruments: Are we there yet? J Surg Res 2014;189:193–197.
33. Basterzi Y, Ersoz G, Sarac G, *et al.* In-vitro comparison of antimicrobial efficacy of various wound dressing materials. Wounds 2010;22:165–170.

Address correspondence to:
Jonathan Steven Alexander
Department of Molecular and Cellular Physiology
Louisiana State University Health Sciences Center
1501 Kings Highway
Shreveport, LA 71103

E-mail: jalexa@lsuhsc.edu